

Supplementary Information

Facile synthesis of Uniform N-doped Carbon-Coated TiO₂ Hollow Spheres with Enhanced Lithium Storage Performances

Mengna Fan^a, Zhonghu Yang^a, Zhihua Lin^a, Xunhui Xiong^{a,*}

^a Guangzhou Key Laboratory of Surface Chemistry of Energy Materials, New Energy Research Institute, School of Environment and Energy, South China University of Technology, Guangzhou 510006, China

1. Experimental

1.1. Method

Synthesis of TiO₂ hollow spheres: TiO₂ hollow spheres are synthesized through the ‘wet conversion’ method. In our experiment, 1 ml industrial titanyl sulfate solution ($c(\text{TiOSO}_4) = 480 \text{ g L}^{-1}$, $c(\text{Fe}^{2+}) = 48 \text{ g L}^{-1}$, $c(\text{Mn}^{2+}) = 0.77 \text{ g L}^{-1}$) used in our previous work¹, and 18 g H₂SO₄ ($c(\text{H}^+) = 1 \text{ mol L}^{-1}$) were added in 800 mL deionized water at 35 °C. Then, 0.1 g Al powder (50-200 nm in diameter, Hongwu New Material) was added and stirred for 3 hours until the solution turned from dark gray to light gray. After filtrating and drying, the sample was added to the 50 mL NaOH (0.2 mol L⁻¹) in 500 mL deionized water and stirred overnight. Finally, TiO₂ hollow sphere was obtained by filtration and drying process.

Synthesis of TiO₂@C materials: TiO₂ precursors were dispersed in Tris-buffer solution (0.1 M, 100 mL) by sonication, and then 0.1 g dopamine hydrochloride were added and stirred for 3 hours at room temperature. After centrifuging and washing with deionized water and ethanol for three times, respectively, the sample was collected and further dried at 60 °C overnight. Finally, the precursors were obtained by annealing at 400 °C for 3 h in an Ar/H₂ atmosphere.

1.2. Material characterization

The X-ray diffraction measurements were conducted on Rigaku D/max 2500 using

Cu Ka radiation and the 2θ range of tests was from the range of 10° - 90° . Raman and XPS measurement were performed by Renishaw RM1000 micro spectroscopic system and Thermo K-Alpha XPS spectrometer respectively. Thermogravimetric analysis (TGA) was performed in the air with the temperature range from 30°C to 800°C . The materials morphologies were measured by FESEM (Hitachi S-4800) and TEM (JEM-2010 JEOL, 200 kV). Brunauer-Emmett-Teller (BET) specific surface areas were obtained using a JW-BK200C Surface Area and Pore size Analyzer (Beijing JWGB Sci. & Tech. Co., Ltd) at the liquid-nitrogen boiling point (77 K).

1.3. Electrochemical measurements

The lithium storage performances of all samples were characterized by fabricating CR2032 coin-type half-cells in an Ar glove box. The anode electrode was prepared by mixing the active material with super P and polyvinylidene fluoride (PVDF) according to a mass ratio of 6:2:2 in N-methyl-2-pyrrolidone. The obtained slurry was cast onto a copper (Cu) foil and then dried at 110°C under vacuum for 12 h. Generally, the mass loading of the active material is about packing density of $\sim 0.5\text{ mg cm}^{-2}$. A solution of 1 M LiPF_6 in EC: DMC: EMC=1:1:1 Vol% is selected as the electrolyte. CV measurements were carried out by a CHI660E electrochemical workstation. LAND-BT2013A measurement system is responded for testing cycling performance and rate capacity at 25°C .

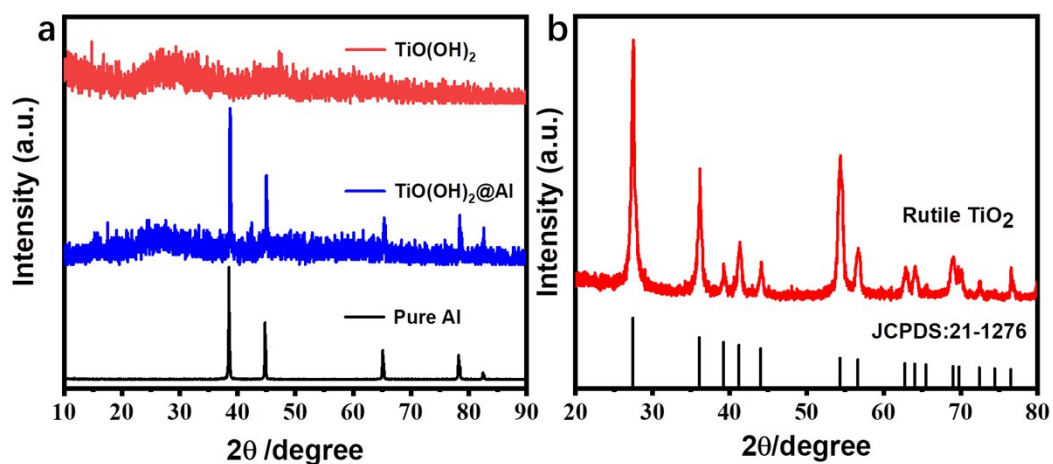


Fig. S1 XRD patterns of precursors at different stages (a) and TiO_2 (b) annealed at $700\text{ }^\circ\text{C}$.

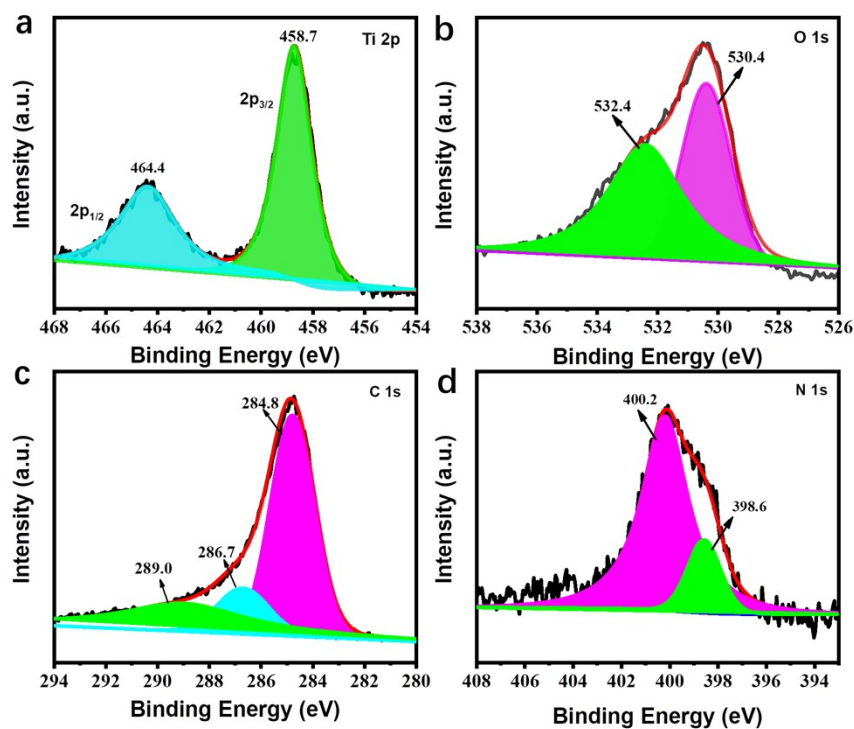


Fig. S2 High resolution XPS spectra of Ti 2p (a), O 1s (b), C 1s (c), N 1s (d) in $\text{TiO}_2@\text{C}$, respectively.

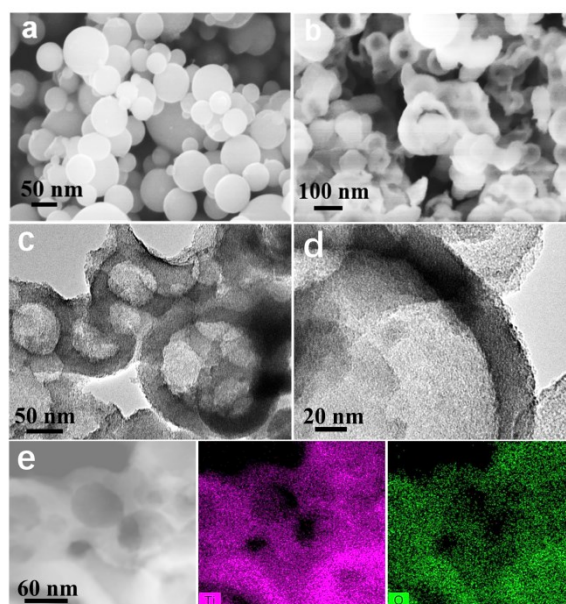


Fig. S3 SEM images of (a) Al powers, (b) TiO(OH)₂@Al; (c)-(d) TEM images of pure TiO₂; (e) elemental mapping images of Ti and O of TiO₂ hollow spheres.

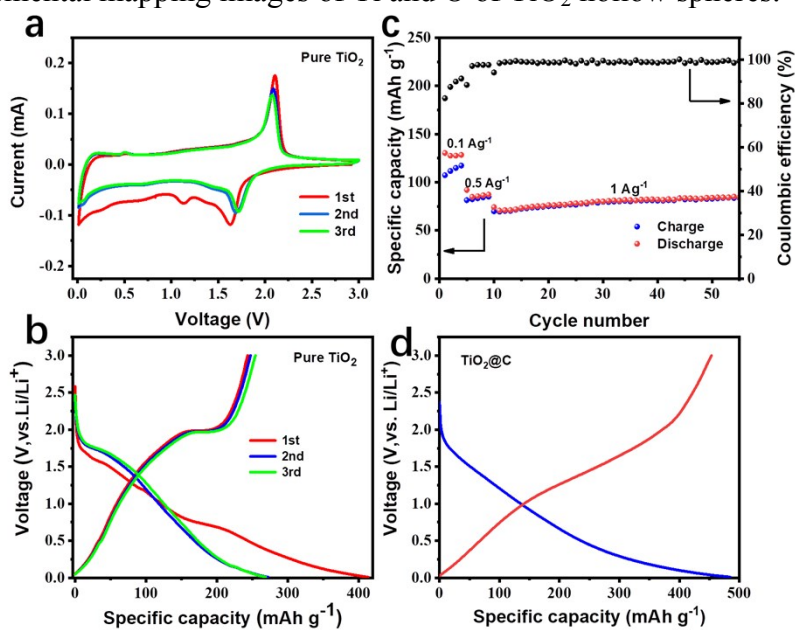


Fig. S4 (a) Cyclic voltammogram of pure TiO₂ at a scanning rate of 0.2 mV s⁻¹; (b) Charge/discharge curves of pure TiO₂ at 0.1 A g⁻¹; (c) the rate capability and the cycle performances of rutile TiO₂; (d) the initial charge-discharge curve of TiO₂@C after chemical prelithiation.

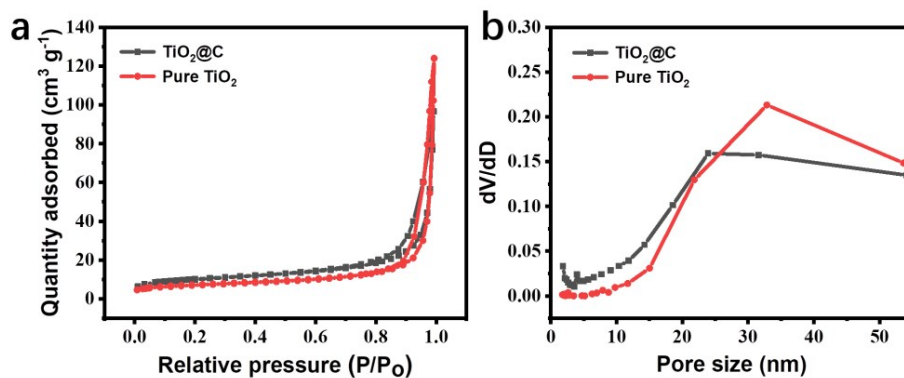


Fig. S5 (a) Nitrogen adsorption/desorption isotherms of TiO_2 and $\text{TiO}_2@\text{C}$; (b) Barrett-Joyner-Halenda (BJH) pore size distribution curves for TiO_2 and $\text{TiO}_2@\text{C}$.

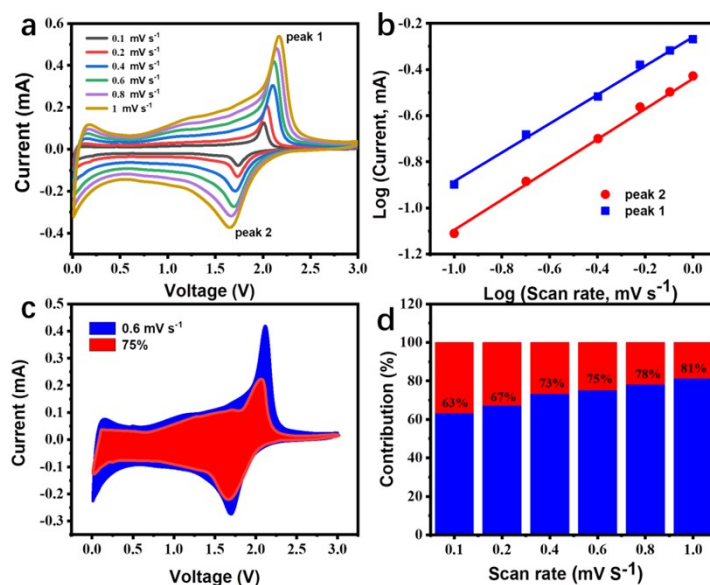


Fig. S6 (a) CV curves of TiO_2 at different scan rates; (b) $\text{Log}(i)$ versus $\text{log}(v)$ plots at different cathodic/anodic peaks for TiO_2 ; (c) Contribution of the surface-driven process at 0.6 mV s^{-1} in TiO_2 ; (d) Capacitance contribution of TiO_2 at different scan rates.

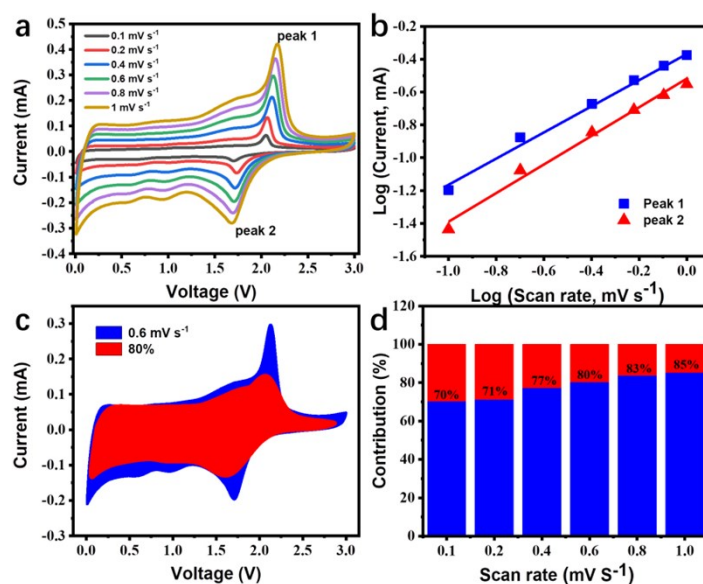


Fig. S7 (a) CV curves of $\text{TiO}_2@\text{C}$ at different scan rates; (b) $\text{Log}(i)$ versus $\text{log}(v)$ plots at different cathodic/anodic peaks for $\text{TiO}_2@\text{C}$; (c) Contribution of the surface-driven process at 0.6 mV s^{-1} in $\text{TiO}_2@\text{C}$; (d) Capacitance contribution of $\text{TiO}_2@\text{C}$ at different scan rates.

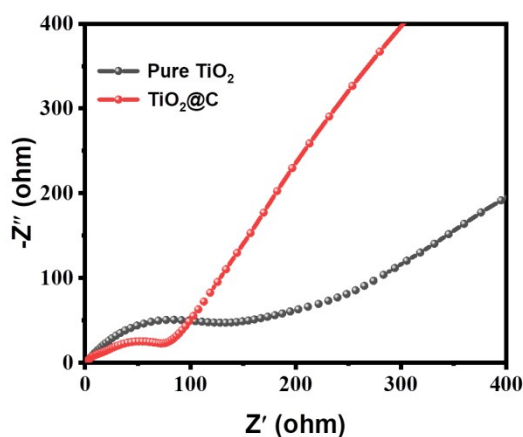


Fig. S8 EIS of pure TiO_2 and $\text{TiO}_2@\text{C}$ after 3 cycles at 0.1 A g^{-1} .

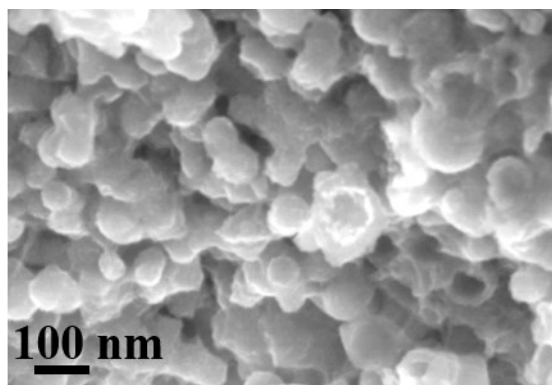


Fig. S9 SEM image of $\text{TiO}_2@\text{C}$ composites after 2000 cycles.

Reference

1 F. Wu, Z. Wang, X. Li, L. Wu, X. Wang, X. Zhang, Z. Wang, X. Xiong, H. Guo, *J. Alloys Compd.*, 2011, **509**, 596-601.